ELSEVIER

1 November 1995

Optics Communications 120 (1995) 264–268

OPTICS COMMUNICATIONS

The transition probability of ^5D_J–$^7F_0$ and hole-burning quantum efficiency in the $Sr_yBa_{1-y}FCl_{0.5}Br_{0.5}:Sm^{2+}$ system

Hongwei Song, Jiahua Zhang, Diankun Gao, Shihua Huang, Jiaqi Yu

Laboratory of Excited State Processes, Changchun Institute of Physics, Chinese Academy of Science, Changchun, 130021, China

Received 21 March 1995; revised version received 1 June 1995

Abstract

We report the changes of the ^5D_J–$^7F_0$(J = 2, 1, 0) transition probability with composition y and its effect on the hole burning quantum efficiency in the $Sr_yBa_{1-y}FCl_{0.5}Br_{0.5}:Sm^{2+}$ system. We observed that the ^5D_J–$^7F_0$ transition probability increases with the increase of Sr concentration. This result is attributed to the reduction of the energy separation between the ^5D_J level and the 4f5d bands, which makes the electron wave functions of ^5D_J states mix further with that of the 4f5d states. The dependence of the hole-burning quantum efficiency on the $5D_J$–$^7F_0$ transition probability was derived by the dynamical equations of the spectral hole burning of divalent samarium. Furthermore, the hole-burning experiments in $SrFCl_{0.5}Br_{0.5}:Sm^{2+}$ and $BaFCl_{0.5}Br_{0.5}:Sm^{2+}$ were performed under the same conditions. The experimental results present that the hole-burning quantum efficiency of $SrFCl_{0.5}Br_{0.5}:Sm^{2+}$ is higher than that of $BaFCl_{0.5}Br_{0.5}:Sm^{2+}$.

1. Introduction

In recent years, much research work has been performed on spectral hole-burning (SHB) of Sm^{2+} since the first observation of photon-gated spectral hole-burning in $BaFCl:Sm^{2+}$ at 2 K was reported in 1985 [1] and hole-burning at 77 K in $BaF(Cl,Br):Sm^{2+}$ was first reported in 1989 [2]. One of the important reasons is that hole-burning of Sm^{2+} has a potential use in frequency domain optical storage (FDOS). Hole-burning of Sm^{2+} has some useful properties compared to the other materials for SHB. Especially, room temperature hole-burning of Sm^{2+} has been realized at present [3–7]. However, there are some problems to be solved in order to apply SHB in FDOS. One of the problems is how to increase the absorption cross section from $^7F_0$ to ^5D_J which is a hole-burning transition. f–f transitions of rare earth ions are electric-dipole-parity forbidden transitions. But it is found that most of emissions of rare earth ions are electric-dipole transitions in experiments. In the light of the theory of Judd–Ofelt [8,9], the reason is that opposite–parity states are mixed into $4f^n$ states. In $Sr_yBa_{1-y}FCl_{0.5}Br_{0.5}:Sm^{2+}$, transitions of $^7F_0$–4f5d are $4f^6$–$4f^55d$ electric-dipole-parity allowed transitions, they have a large absorption cross section and high excitation efficiency. So it is possible to increase the excitation efficiency of $^7F_0$–^5D_J if we can make the ^5D_J levels nearer to the 4f5d bands so that the wave functions of ^5D_J are mixed further with that of 4f5d bands.

The paper reports studies on the dependence of the $^5D_J-{}^7F_0$ transition probability on composition (y) in $Sr_yBa_{1-y}FCl_{0.5}Br_{0.5}:Sm^{2+}$ and its effect on hole-burning efficiency.

SSDI 0030-4018(95)00428-9

2. Experimental

The powder samples of $Sr_yBa_{1-y}FCl_{0.5}Br_{0.5}:Sm^{2+}$ ($y=0$, 0.25, 0.5, 0.75, 1.0) were prepared by the method described in Ref. [9].

The excitation spectra of Sm^{2+} were measured by monitoring the energy position of 688 nm with a Hitachi F-4000 spectrometer. Fluorescent spectra and the fluorescent decay curves were measured with a nitrogen laser, and samples were put into a helium gas closed-cycling cryostat. A D330 monochromator, a Boxcar averager and a Datemate micro-computer were used to detect and analyze fluorescence of this series of samples. In hole-burning experiments, the samples were pumped and gated by a Nd:YAG laser.

3. Results and discussion

3.1. The energy separation between the 4f5d bands and the ^5D_J level

Fig. 1 shows the 4f5d bands in the excitation spectra of $BaFCl_{0.5}Br_{0.5}:Sm^{2+}$ and $SrFCl_{0.5}Br_{0.5}:Sm^{2+}$ at room temperature. It shows that there are four excitation peaks for each 4f5d bands in the $Sr_yBa_{1-y}FCl_{0.5}Br_{0.5}:Sm^{2+}$ series and the peaks 'a' which are nearest to ^5D_J level shift to the low energy side with the increase of Sr concentration. The total move is about 8 nm from $BaFCl_{0.5}Br_{0.5}:Sm^{2+}$ to $SrFCl_{0.5}Br_{0.5}:Sm^{2+}$. The other excitation spectra in $Sr_yBa_{1-y}FCl_{0.5}Br_{0.5}$ series ($y=0.25$, 0.5, 0.75) were obtained and in accord with this rule also. With the increase of Sr concentration, the position of the ^5D_J level shift to the low energy side also. Table 1 shows energy positions (cm^{-1}) of the peaks 'a' and that of the ^5D_J ($J=0,1,2$) emission peaks, the energy interval between peaks 'a' and the $^5D_J-{}^7F_0$ ($J=0$, 1, 2) emission peaks. Table 1 shows that the ^5D_J level and the 4f5d bands move to the low energy side with the increase of Sr concentration and the shift of the 4f5d bands is more significant comparing to that of the ^5D_J level. So the separation between the 4f5d bands and the ^5D_J level becomes smaller with the increase of the Sr concentration.

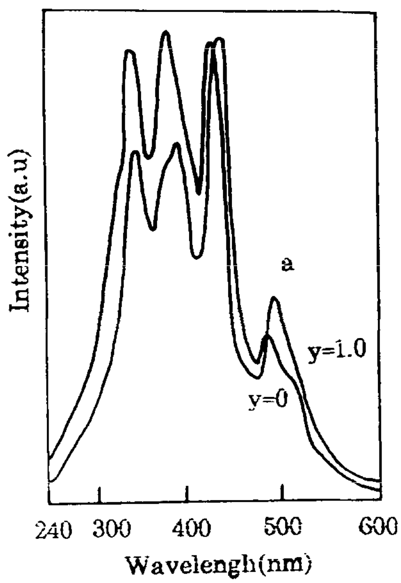

Fig. 1. Excitation spectra of $Sy_yBa_{1-y}FCl_{0.5}Br_{0.5}:Sm^{2+}$ measured by monitoring the $^5D_0-{}^7F_0$ emission and scanning the range of 4f5d bands (a) $y=0$, (b) $y=1.0$.

Table 1
Energy position (cm^{-1}) of the peak 'a' which is at the longest wavelength of 4f5d bands and that of $^5D_2$, $^5D_1$ and $^5D_0$ emission peaks. The energy separation between peak 'a' and $^5D_2$, $^5D_1$, $^5D_0$ emission peaks.

E	y				
	1.0	0.75	0.5	0.25	0
E_a	20566	20640	20683	20790	20877
E_2	17757	17778	17787	17804	17818
E_1	15824	15844	15864	15872	15876
E_0	14478	14496	14516	14524	14531
ΔE_{a2}	2809	2862	2905	2986	3059
ΔE_{a1}	4742	4796	4819	4918	5001
ΔE_{a0}	6088	6144	6167	6266	6346

3.2. The ^5D_J–$^7F_0$ electron transition probabilities of Sm^{2+} in $Sr_yBa_{1-y}FCl_{0.5}Br_{0.5}:Sm^{2+}$ series

In the light of the theory of Judd-Ofelt, if $|\Psi'J'J'_z\rangle$ is a state of the ^5D_J level, $|\Psi''\rangle$ is a state of the 4f5d bands, the mixed state $|B\rangle$ of the ^5D_J level is

$$|B\rangle = |\Psi'J'J'_z\rangle + \sum_{\Psi''} \frac{|\Psi''\rangle\langle\Psi''|H_c|\Psi'J'J'_z\rangle}{E(\Psi'J'J'_z) - E(\Psi'')}$$

where H_c is hamiltonian of the interaction to produce the mixture of wave functions. If $\langle A| = \langle\Psi JJ_z|$ is a state of $^7F_0$, the matrix elements of electric dipole P are

$$\langle A|P|B\rangle = \sum_{\Psi''} \frac{\langle \Psi JJ_z|P|\Psi''\rangle \langle \Psi''|H_c|\Psi'J'J'_z\rangle}{E(\Psi'J'J'_z) - E(\Psi'')}$$

since $|\Psi''\rangle$ is the state of the 4f5d bands, $\langle \Psi JJ_z|P|\Psi''\rangle$ is the parity allowed matrix element. The smaller the value of $[E(\Psi'J'J'_z) - E(\Psi'')]$, the larger the value of the ^5D_J–$^7F_0$ transition probability.

In order to obtain the ^5D_J–$^7F_0$ electron transition probability, the ^5D_J–$^7F_0$ fluorescence decay times at different temperatures were measured. Table 2, Table 3 and Table 4 are the variations of the ^5D_J ($J=2$, 1, 0)–$^7F_0$ decay times on composition (y) and temperature, respectively. Table 2 shows that the $^5D_2$–$^7F_0$ decay times approach saturation values at temperatures below 30 K and they are shortened with the increase of temperature. Above 100 K, the $^5D_2$–$^7F_0$ fluorescence is difficult to be detected. In the light of the theory of multi-phonon relaxation: $\tau = 1/(W_{NR} + W_R)$, where W_{NR} is the nonradiative transition probability of ^5D_J and W_R is the radiative transition probability of ^5D_J–$\Sigma_{J'}$ $^7F_{J'}$. The radiative transition decreases with the decrease of temperature, if T approaches 0, then W_{NR} approaches 0. But the radiative transition probability does not change with temperature. Therefore, the result above shows that the nonradiative transition of $^5D_2$ is negligible compared to that of the ^5D_J–$\Sigma_{J'}$$^7F_{J'}$ radiative transition at a temperature below 30 K. In that case, the ^5D_J–$\Sigma_{J'}$ $^7F_J{}'$ radiative transition probability equals $1/\tau_0$. τ_0 is the $^5D_2$–7F_0 decay time when τ_0 approaches saturation value at low temperature. The decay times of $^5D_1$–$^7F_0$ and $^5D_0$–$^7F_0$ were measured to 300 K. To the samples of some value of y, the decay times of $^5D_0$–$^7F_0$ approach a saturation value at temperatures below 30 K, they increase with the increase of temperature to a certain temperature and then decrease with the increase of temperature above this temperature. These facts can be explained in the light of the luminescent dynamic equations [10]. By the same method as above, the electron transition probabilities of $^5D_1$–$\Sigma_{J'}$ $^7F_{J'}$ and $^5D_0$–$\Sigma_{J'}$ $^7F_{J'}$ were obtained. So we obtain the dependence of the transition probability of ^5D_J–$\Sigma_{J'}$ $^7F_{J'}$ ($J=2$, 1, 0) on the value of y (see Fig. 2). It shows that the ^5D_J–$\Sigma_{J'}$ $^7F_{J'}$ transition probability increases with the increase of the Sr concentration in $Sr_yBa_{1-y}FCl_{0.5}Br_{0.5}:Sm^{2+}$ series. From Fig. 2 we can see that, the increase in R for the $^5D_2$, $^5D_1$ and $^5D_0$ level are about 17%, 47% and 18% respectively, and we cannot find a systematic relationship between the amount of increment in R and the energy separations ΔE_{ai} ($i=0$, 1, 2) in Table 1. We think that the hamiltonian of interaction to produce the mixture of wave functions is different for the $^5D_2$, $^5D_1$ and $^5D_0$ level, hence the amount of increment in R is complex. In the experiments, the relative intensity of ^5D_y–$^7F_{J'}$ almost

Table 2
Variation of the $^5D_2$ fluorescent lifetime (ms_{-1}) in $Sr_yBa_{1-y}FCl_{0.5}Br_{0.5}:Sm^{2+}$ on composition (y) and temperature.

T(K)	y				
	1.0	0.75	0.5	0.25	0
17	0.36	0.38	0.40	0.43	0.46
30	0.35	0.39	0.39	0.44	0.47
40	0.15	0.16	0.24	0.29	0.27
50	0.02	0.02	0.04	0.04	0.21
70	0.01	0.01	0.01	0.02	0.06

Table 3
Variation of the $^5D_1$ fluorescent lifetime (ms_{-1}) in $Sr_yBa_{1-y}FCl_{0.5}Br_{0.5}:Sm^{2+}$ on composition (y) and temperature.

T(K)	y				
	1.0	0.75	0.5	0.25	0
17	0.43	0.61	0.67	0.72	0.89
30	0.42	0.62	0.68	0.70	0.88
50	0.40	0.51	0.61	0.61	0.76
70	0.38	0.49	0.60	0.60	0.78
100	0.35	0.52	0.55	0.40	0.65
150	0.32	0.36	0.26	0.30	0.64
200	0.24	0.35	0.22	0.28	0.64
250	0.17	0.17	0.15	0.20	0.64

Table 4
Variation of the $^5D_0$ fluorescent lifetime (ms^{-1}) in $Sr_yBa_{1-y}FCl_{0.5}Br_{0.5}:Sm^{2+}$ on composition (y) and temperature.

T(K)	y				
	1.0	0.75	0.5	0.25	0
17	1.44	1.67	1.76	1.87	1.89
30	1.38	1.69	1.74	1.89	1.89
50	1.32	1.69	1.85	1.86	2.07
70	1.31	1.58	1.43	1.90	2.05
100	1.32	1.28	1.40	1.44	2.31
150	1.30	1.31	1.28	1.46	1.71
200	1.05	1.09	1.15	1.14	1.68
250	1.02	0.86	0.72	1.05	1.61

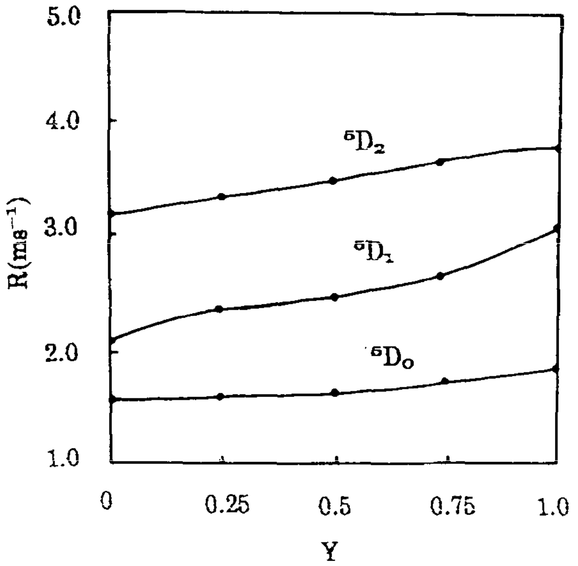

Fig. 2. Dependence of $^5D_J - \Sigma_{J'}\, ^7F_{J'}$ ($J = 0, 1, 2$) radiative transition probability in $Sr_yBa_{1-y}FCl_{0.5}Br_{0.5}:Sm^{2+}$.

does not change with change of y, so the ^5D_J–$^7F_0$ transition probability is proportional to the ^5D_J–$\Sigma_{J'}\, ^7F_{J'}$ transition probability. According to the Einstein equation:

$$R' = 8\pi h\nu^3 R/c^3 ,$$

where R' is the absorption probability. So we can derive the $^7F_0$–^5D_J absorption probability which is an important parameter for hole-burning efficiency.

3.3. The effect of the $^7F_0$–^5D_J absorption probability on hole-burning efficiency

Under the condition of $\mu \leqslant \tau \leqslant T_0$ (μ is the width of the laser pulse, τ is the electron lifetime of the ^5D_J level, T_0 is the interval of the laser pulses) an approximate solution was derived by the dynamical equations of the three energy level system for hole-burning in the ^5D_J–$^7F_0$ transition with a pulsed laser. It is as follows [11]:

$$N_3(n) = \eta_{23} I I' \sigma_0 \sigma_1 \mu \tau' N_0 \exp[a(n-1)] ,$$

where N_3 is the number of electrons captured by traps in the nth pulse. η_{23} is the probability that traps capture electrons from the conduction band, there η_{23} is taken as a constant. I and I' are the intensities of hole-burning laser and the gating laser, respectively. σ_0 and σ_1 are the $^7F_0$–$^5D_2$ and the $^5D_2$–4f5d absorption cross sections, respectively. τ' is the electron lifetime of the conduction band. N_0 is the $^7F_0$ electron populations. $a = \ln(1 - \eta_{23} I I' \sigma_0 \sigma_1 \mu \tau')$. $n = 0, 1, 2\ldots$, etc.

The hole-burning quantum efficiency η is defined as the number of traped electrons produced by a hole-burning photon when t approaches 0, so

$$\eta = N_3 h\omega / I\mu = \eta_{23} \sigma_0 \sigma_1 I' \tau' N_0 h\omega .$$

Since σ_0 is proportional to the $^7F_0 - {}^5D_J$ absorption probability R', the hole-burning quantum efficiency η is proportional to R'. Because the ^5D_J fluorescence lifetime is in order of ms, and the pulse width (the gating time in a pulse) is in order of ns, the change of the ^5D_J lifetime has little effect on the photon gating process. Furthermore, the absorption probability of the ^5D_J-conduction band is much larger than that of $^7F_0$–^5D_J, most of the electrons in the ^5D_J level are gated to the conduction band. Hence we think that the $^7F_0$–^5D_J transition probability is the most important factor for hole burning efficiency.

Therefore, in the case of weak excitation pumped and gated by a pulsed laser, since the $^7F_0$–^5D_J absorption probability of $Sr_yBa_{1-y}FCl_{0.5}Br_{0.5}:Sm^{2+}$ increases with the increase of Sr concentration, the hole-burning quantum efficiency performed in the $^7F_0$–^5D_J transition is expected to be enhanced with the increase of Sr concentration.

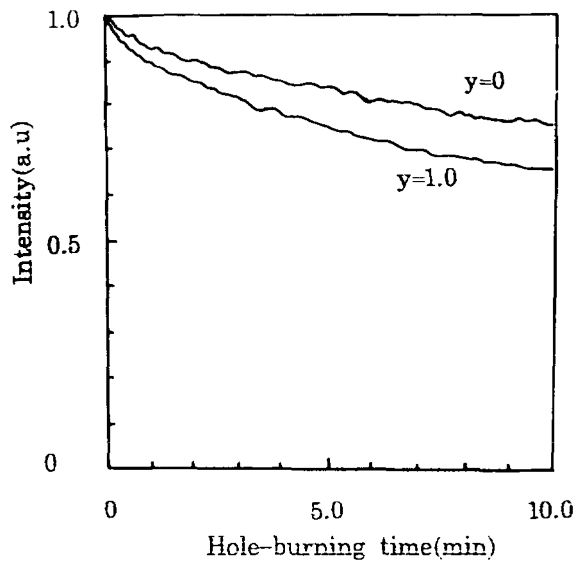

Fig. 3. Dependence of $^5D_2 - {}^7F_0$ fluorescence intensities of Sm^{2+} ions at burning site (at 77 K) on hole-burning time (hole-burning of $^5D_2 - {}^7F_0$ were performed in same condition. $I_{hole} = 80$ mJ).

In order to prove our theoretical result, the hole-burning experiments were performed in $SrFCl_{0.5}Br_{0.5}:Sm^{2+}$ and in $BaFCl_{0.5}Br_{0.5}:Sm^{2+}$ by a 560 nm pulsed laser at 77 K. Fig. 3 shows the dependence of the $^5D_2$ emission intensities at a burning site on hole-burning time in the same hole-burning condition. It shows that a deeper hole can be obtained in $SrFCl_{0.5}B4_{0.5}:Sm^{2+}$ under the same hole-burning condition ($I_{hole} = 80$ mW) and at the same hole-burning time. So we can claim that the hole-burning quantum efficiency in $SrFCl_{0.5}Br_{0.5}:Sm^{2+}$ is larger than in $BaFCl_{0.5}Br_{0.5}:Sm^{2+}$ if we suppose that the change of y has little effect on the other parameters except the $^7F_0$–^5D_J absorption probability. The experimental results is in accord with the theoretical result.

4. Conclusions

In the $Sr_yBa_{1-y}FCl_{0.5}Br_{0.5}:Sm^{2+}$ series, the higher the concentration of Sr, the smaller the energy separation between the ^5D_J level and the 4f5d bands, the larger the ^5D_J–$^7F_0$ transition probability. In the process of photon-gated spectral hole-burning pumped and gated by a pulsed laser, the hole-burning quantum efficiency is proportional to the $^7F_0 - {}^5D_J$ transition probability. The experimental results show that the hole-burning quantum efficiency increases with the increase of Sr concentration.

References

[1] A. Winnaker, R.M. Shelby and R.M. Macfarlane, Optics Lett. 10 (1985) 350.
[2] C. Wei, S. Huang and J. Yu, J. Lumin. 43 (1989) 161.
[3] J. Zhang, S. Huang and J. Yu, Chinese J. Lumin. 12 (1991) 181.
[4] K. Holloday, C. Wei, M. Croci and Urs. P. Wild, J. Lumin. 53 (1992) 227.
[5] J. Zhang, S. Huang and J. Yu, Optics Lett. 17 (1992) 149.
[6] R. Jaaniso and H. Bill. Euro, Phys. Lett. 16 (1991) 569.
[7] K. Horie, S. Todoriki and N. Soga, J. Lumin. 55 (1993) 217.
[8] B.R. Judd, Phys. Rev. 127 (1962) 719.
[9] G.R. Ofelt, J. Chem. Phys. 37 (1962) 511.
[10] H. Song, J. Zhang, S. Huang and J. Yu, Chinese J. Lumin. 3 (1994) 201.
[11] H. Song, J. Zhang, S. Huang and J. Yu, Chinese J. Lumin. 3 (1994) 216.